Supporting Information for "Hierarchical Structure and Polymorphism of a Sphere-Cubic Shape Amphiphile Based on a Polyhedral Oligomeric Silsesquioxane-[60]Fullerene Conjugate"

Hao-Jan Sun,[a] Yingfeng Tu,[b,] Chien-Lung Wang,[a] Ryan M. Van Horn,[a] Chi-Chun Tsai,[a] Matthew J. Graham,[a] Bin Sun,[c] Bernard Lotz,[d] Wen-Bin Zhang,[a,]* and Stephen Z.D. Cheng[a,]**

[1]College of Polymer Science and Polymer Engineering, Department of Polymer Science,
The University of Akron, Akron, OH, USA 44325

[2]College of Chemistry, Chemical Engineering and Materials Science, Soochow University,
Suzhou 215123, China

[3]State Key Lab for Chemical Fibers & Polymer Materials, Donghua University,
Shanghai, 201620 China

[4]Institut Charles Sadron, 23, Rue du Loess, Strasbourg 67034, France

1. ^{1}H and ^{13}C NMR of POSS-C_{60} (3)

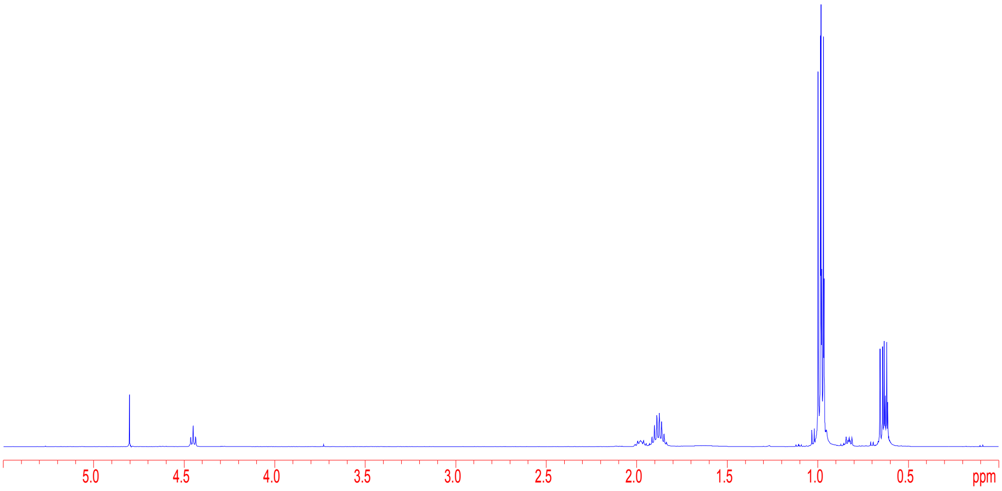

Figure S1. ^{1}H NMR spectrum of POSS-C_{60} (**3**).

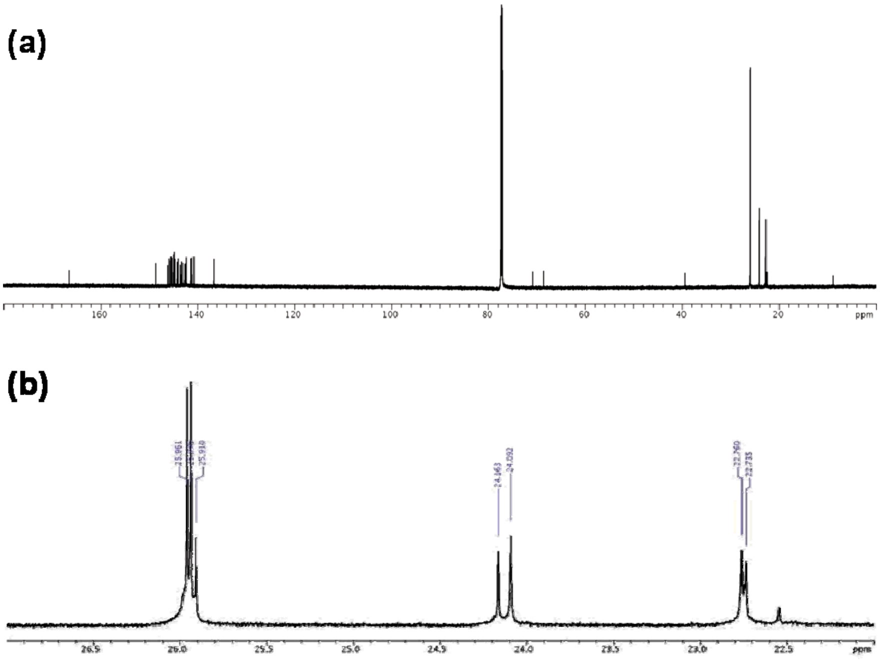

Figure S2. (a) ^{13}C NMR spectrum of POSS-C_{60} (**3**). (b) Enlarged spectrum from (a) for the *i*-butyl groups connected to POSS cage with chemical shifts between 22.7 to 26.0 ppm

2. HSQC NMR Experiments and Additional Discussions

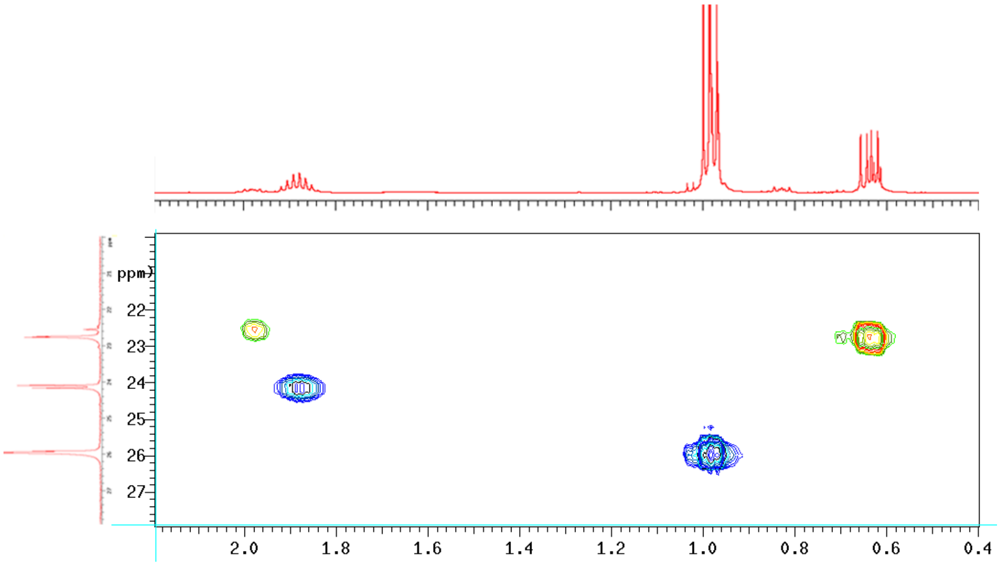

Figure S3. HSQC NMR figure of POSS-C$_{60}$ (**3**).

Figure S3 is the HSQC NMR spectrum for the POSS-C$_{60}$ (**3**) in CDCl$_3$ solution with chemical shift in ^{1}H NMR on the *x*-axis and ^{13}C NMR on the *y*-axis. The peaks in HSQC NMR indicate hydrogen atoms which are directly connected to each carbon. The warm colors (green and red) indicate methene groups, while the cold colors (blue) indicate methyl and methenyl groups. By comparing with the corresponding chemical shift in the ^{1}H NMR spetrum, we can identify the peaks for *i*-butyl groups: resonance at δ 25.961, 25.936, 25.910 for the methyl groups; δ 24.163, 24.092 for the methenyl groups; and δ 22.760, 22.735 for methene groups. When there are eight identical arms connected to each corner of the POSS cage, the molecule possesses O_h symmetry. If one arm was substituted by other functional group, the molecule symmetry was broken to C_{3v} with the C$_3$ axis going through the substituted silicone and parallel to the body diagonal of the POSS cage. The seven arms are thus separated into three groups. Theoretically, nine peaks should be observed for *i*-butyl groups, three for methyl groups, three for methene groups, and another three for methenyl groups. The three peaks for the methyl groups were indeed observed. However, only two peaks were observed for both methene groups and methenyl groups, which is probably due to the limited resolution of the instrument since the difference of the chemical shifts is very small.

3. MALDI-TOF Mass Spectrum

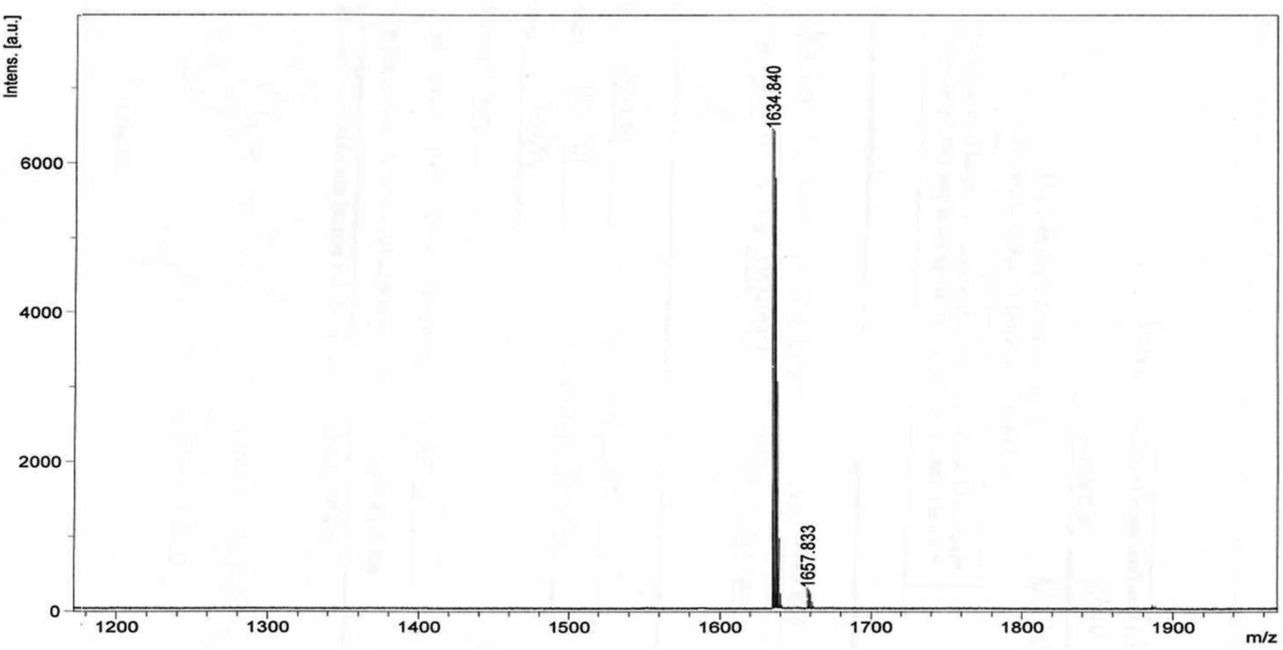

Figure S4. MALDI-TOF Mass spectrum of POSS-C_{60} (**3**). The first peak corresponds to the molecular peak ($[M]^+$) and the second one is the one with sodium ion ($[M{\cdot}Na]^+$).

4. FT-IR spectrum and UV-vis Absorption Spectrum

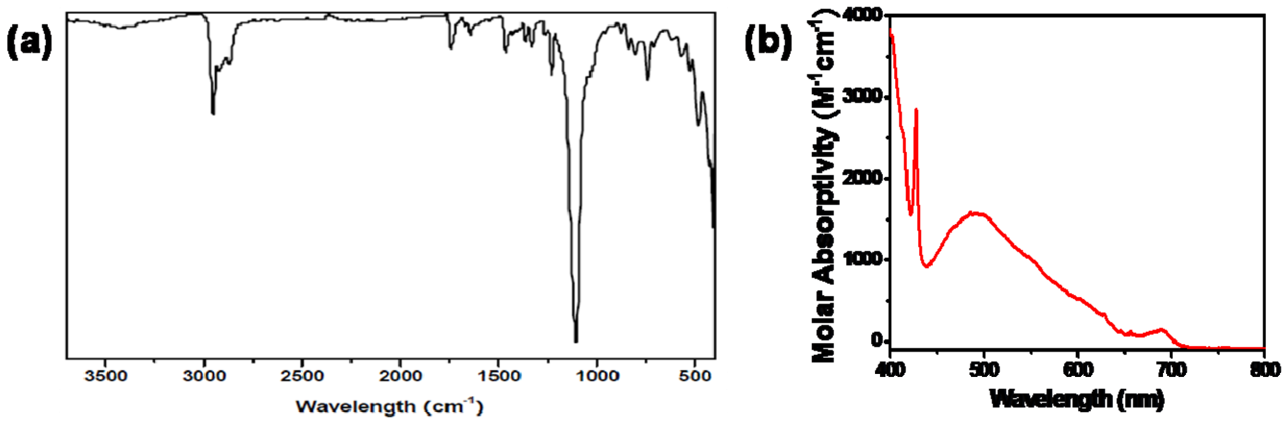

Figure S5. FT-IR spectrum (a) and UV-vis spectrum (b) of POSS-C_{60} (**3**) at room temperature in chloroform.

Figure S5b is the UV-vis. absorption spectrum of POSS-C_{60} (**3**) in chloroform at room temperature. The small peak at 690 nm with a molar absorptivity of 220 M^{-1} cm^{-1} and the sharp peak at 427 nm with a molar absorptivity of 2840 M^{-1} cm^{-1} are the characteristic features in the spectra for methano[60]fullerenes. The absorption spectrum remains nearly the same in solvents of different polarities. The peak position and absorptivity are similar to that of other fullerene derivatives found in literature.[1] These similarities indicate that the absorption is dictated by the electronic structure of the methano[60]fullerene moiety with similar energies and transition probabilities with little influence of solvent. It confirms that the functionalization of the C_{60} has not dramatically altered its electronic and optical properties.

5. Thermal Gravimetric Analysis

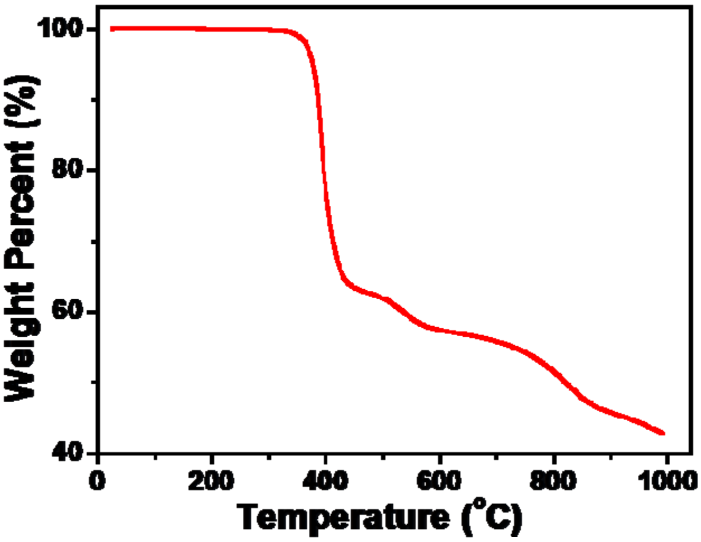

Figure S6. TGA diagram of POSS-C_{60} (**3**).

Thermal gravimetric analysis (Figure S6) shows very good thermal stability for POSS-C_{60} (**3**) with a 0.5% weight loss at 341 °C. This temperature represents the decomposition of the spacer linked between POSS and fullerene and subsequent sublimation of the POSS cages.[2,3] Even when the materials was heated to 800 °C, the POSS-C_{60} (**3**) has more than 50% weight remaining.

6. Supporting Data for Solid-state Crystal Structure Determination:

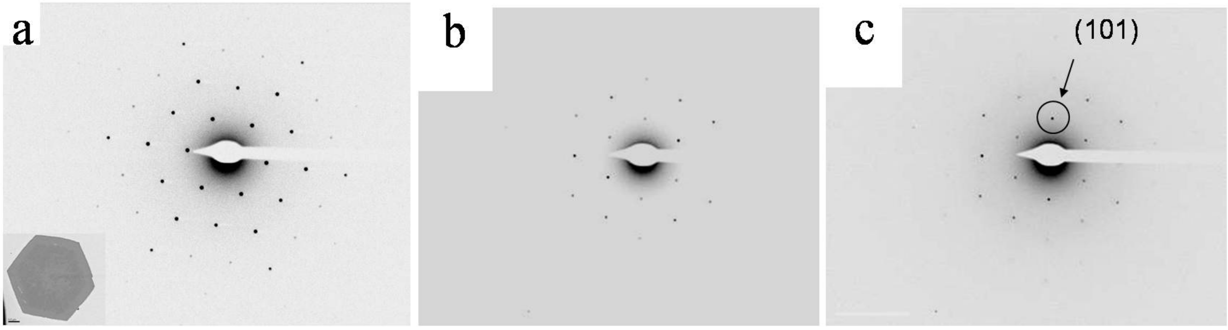

Figure S7. (a) TEM BF image and ED pattern of POSS-C_{60} (**3**) single crystal with a hexagonal lattice. (b) ED pattern of POSS-C_{60} (**3**) at a 8° tilt along *b*-axis, and (c) ED pattern of POSS-C_{60} (**3**) at a 12° tilt along the *b*-axis.

The *c*-axis length of hexagonal crystal can be determined by tilted ED experiments in TEM (Figure S7). In Figure S7b, The (100) spot almost disappeared when the tilting angle reached θ8º along the *b*-axis, and the (101) spot appeared when the crystal tilted 12º along the *b*-axis (Figure S7c). The d-spacing of the (101) plane was measured to be 0.86 nm, and the length of *c*-axis can thus be determined as 4.27 nm. The correct angle between the plane (100) and (101) was calculated as 11.7°.

The calculated and observed d-spacing and 2 θ angle for the two crystal structures are summarized in Table S1 and Table S2 for comparison.

Table S1. Crystallographic Parameters of Type I Orthorhombic Crystals

		2θ (deg)		*d*-spacing (Å)	
no.	(hkl)	exptl[a]	calc[b]	exptl[a]	calc[b]
1	(001)	2.43	2.44	36.35	36.20
2	(002)	4.86	4.88	18.18	18.1
3	(003)	7.29	7.33	12.12	12.07
4	(200)	8.45	8.42	10.46	10.50
5	(201)	8.76	8.77	10.09	10.08

6	(110)	9.37	9.42	9.44	9.39
7	(004)	9.75	9.77	9.07	9.05
8	(210)	11.90	11.92	7.42	7.42
9	(310)	15.22	15.21	5.82	5.82
10	(311)	15.41	15.41	5.75	5.75
11	(312)	16.02	15.98	5.53	5.54
12	(020)	16.85	16.89	5.26	5.25
13	(400)	16.85	16.89	5.26	5.25
14	(021)	17.11	17.07	5.18	5.20
15	(120)	17.42	17.41	5.09	5.09
16	(121)	17.55	17.58	5.05	5.04
17	(023)	18.41	18.43	4.82	4.81
18	(220)	18.85	18.90	4.71	4.70
19	(410)	18.85	18.90	4.71	4.70
20	(221)	19.10	19.06	4.65	4.66
21	(320)	21.11	21.15	4.21	4.20
22	(510)	22.77	22.80	3.91	3.90
23	(600)	25.45	25.45	3.50	3.50
24	(230)	26.88	26.85	3.32	3.32
25	(610)	26.88	26.85	3.32	3.32
26	(330)	28.47	28.51	3.14	3.13
27	(620)	30.65	30.70	2.92	2.91
28	(040)	34.12	34.16	2.63	2.63
29	(630)	36.22	36.30	2.48	2.47

[a] Experimental values observed in both WAXD and TEM (Figure 1 &2). [b] Calculated based on the orthorhombic unit cell of $a = 2.10$nm, $b = 1.05$nm, $c = 3.62$nm, and $\alpha = \beta = \gamma = 90°$.

Table S2. Crystallographic Parameters of Type II Hexagonal Crystals

		2θ (deg)		*d*-spacing (Å)	
no.	(hkl)	exptl[a]	calc[b]	exptl[a]	calc[b]
1	(001)	2.07	2.07	42.70	42.70
2	(002)	4.12	4.14	21.45	21.35
3	(003)	6.19	6.21	14.29	14.23
4	(100)	10.05	10.01	8.80	8.83
5	(110)	17.45	17.39	5.08	5.10
6	(200)	20.05	20.10	4.43	4.42
7	(120)	26.67	26.70	3.34	3.34
8	(210)	26.67	26.70	3.34	3.34
9	(300)	30.30	30.35	2.95	2.94
10	(220)	35.25	35.19	2.55	2.55
11	(400)	40.81	40.86	2.21	2.21

[a]Experimental values observed in both WAXD and TEM (Figure 1 &2). [b]Calculated based on the hexagonal unit cell of a = 1.02nm, b = 1.02nm, c = 4.27nm, $\alpha = \beta = 90°$, and $\gamma = 120°$.

Acknowledgments, The characterizations provided in this supporting information were helped by Dr. Xiaohong Li, Prof. Peter L. Rinaldi, and Prof. Chrys Wesdemiotis at the Department of Chemistry at The University of Akron.

References

1. Ma, B.; Bunker, C. E.; Gudura, R.; Zhang, X.-F.; Sun, Y.-P. *J. Phys. Chem.* **1997**, *101*, 5626-5632.
2. Zhang, C.; Babonneau, F.; Bonhomme, C.; Laine, R. M.; Soles, C. L.; Hristov, H. A.; Yee, A. F. *J. Am. Chem. Soc.* **1998**, *120*, 8380-8391.

3. Mantz, R. A.; Jones, P. F.; Chaffee, K. P.; Litchtenhan, J. D.; Gilman, J. W. *Chem. Mater.* **1996**, *8*, 1250-1259.